

Synthesis of Pentacene Nanotubes by Melt-Assisted Template Wetting

Claire Barrett,[†] Daniela Iacopino,[†] Deirdre O'Carroll,[†]
Gianluca De Marzi,[†] David A. Tanner,[‡]
Aidan J. Quinn,[†] and Gareth Redmond^{*,†}

Nanotechnology Group, Tyndall National Institute,
Lee Maltings, Prospect Row, Cork, Ireland, and Department
of Manufacturing and Operations Engineering & Materials
and Surface Science Institute, University of Limerick,
Limerick, Ireland

Received September 21, 2006

Revised Manuscript Received December 12, 2006

Semiconductor nanowires and nanotubes represent attractive building blocks for “bottom-up” assembled nanoscale electronic and photonic devices.^{1,2} In particular, inorganic semiconductor nanowires and carbon nanotubes have shown great promise because they can potentially function as device components for logic,³ memory,⁴ and sensing applications.⁵ One-dimensional (1-D) nanostructures could also function as interconnects for integrated nanosystems or molecular electronic devices.⁶ Polymers and small organic molecules are attractive materials for (opto-) electronics due to their chemically tunable optical and electronic properties,⁷ as well as their potential for low-cost fabrication of flexible or large area devices.⁸ In particular, pentacene has shown tremendous promise for thin film transistor (TFT) applications,⁹ with reports of hole mobilities approaching $1 \text{ cm}^2 \text{ V}^{-1} \text{ s}^{-1}$ for TFTs fabricated on flexible substrates.^{9d} Recently, a new method for formation of 1-D organic nanotubes and nanowires by wetting of porous anodized alumina membranes

has been reported.^{10a} This method of template wetting has been extended to a broad range of materials, including polymers,¹⁰ small molecules,¹¹ liquid crystals,¹² metals,¹³ ferroelectrics,¹⁴ and multicomponent or heterostructure systems.^{10a,b,13b}

In this work, we report on convenient synthesis of pentacene nanotubes by the method of melt-assisted template wetting and on electrical contacting of single tubes. Briefly, pentacene powder is placed on an alumina pore array and heated above its melting point under an inert atmosphere; see Supporting Information. As a result of the high surface energy of the alumina membrane, a thin surface film will rapidly cover the pore walls in the initial stages of wetting, forming nanotubes with well-defined wall thicknesses.^{10a} Figure 1a shows a scanning electron microscopy (SEM) image of an array of pentacene nanotubes following partial dissolution of the alumina template in aqueous NaOH. The density of nanotubes ($\sim 10^9$ per template) demonstrates the efficiency of the melt-assisted wetting process for high-yield preparation of these novel 1-D nanostructures. Figure 1b shows a high magnification image of the back side of part of the membrane shown in Figure 1a. The large number of protruding nanotubes indicates almost complete filling of the template during melt injection, confirming formation of $\sim 60 \mu\text{m}$ long tubes. Histogram analysis of tube diameters and wall thicknesses measured using SEM yielded mean values for the tube outer diameter ($D \approx 350 \text{ nm}$) and wall thickness ($W \approx 40 \text{ nm}$).

Following synthesis, the nanotubes could be liberated from the template by completely dissolving the alumina in aqueous NaOH and ultimately dispersed in an appropriate solvent following several cycles of washing by sonication and centrifugation. The mean nanotube length measured for dispersed tubes decreased as a function of the number of sonication steps, resulting in a mean wire length $\sim 15 \mu\text{m}$, measured for dispersed single wires following a total of three sonications. Individual tubes with lengths up to $30 \mu\text{m}$ were also observed at low number density (less than 1 in 50).

Figure 2a shows a high-resolution SEM image of a pentacene nanotube drop-deposited on an oxidized silicon

* Corresponding author. E-mail: gareth.redmond@tyndall.ie.

[†] Tyndall National Institute.

[‡] University of Limerick.

- (1) Huang, Y.; Lieber, C. M. *Pure Appl. Chem.* **2004**, *76*, 2051.
- (2) Yao, Z.; Dekker, C.; Avouris, P. *Top. Appl. Phys.* **2001**, *80*, 147.
- (3) (a) Derycke, V.; Martel, R.; Appenzeller, J.; Avouris, P. *Nano Lett.* **2001**, *1*, 453. (b) Huang, Y.; Duan, X.; Cui, Y.; Lathon, L. J.; Kim, K.-H.; Lieber, C. M. *Science* **2001**, *294*, 1313. (c) Bachtold, A.; Hadley, P.; Nakanishi, T.; Dekker, C. *Science* **2001**, *294*, 5545.
- (4) (a) Rueckes, T.; Kim, K.; Joselevich, E.; Tseng, G. Y.; Cheung, C. L.; Lieber, C. M. *Science* **2000**, *289*, 94. (b) Duan, X.; Huang, Y.; Lieber, C. M. *Nano Lett.* **2002**, *2*, 487.
- (5) (a) Kong, J.; Franklin, N. R.; Zhou, C.; Chapline, M. G.; Peng, S.; Cho, K.; Dai, H. *Science* **2000**, *287*, 622. (b) Cui, Y.; Wei, Q.; Park, H.; Lieber, C. M. *Science* **2001**, *293*, 1289. (c) Besteman, K.; Lee, J.-O.; Wiertz, F. G. M.; Heering, H. A.; Decker, C. *Nano Lett.* **2003**, *3*, 727.
- (6) (a) Kovtyukhova, N. I.; Mallouk, T. E. *Chem.—Eur. J.* **2002**, *8*, 4355. (b) Melosh, N. A.; Boukai, A.; Diana, F.; Gerardot, B.; Badolato, A.; Petroff, P. M.; Heath, J. R. *Science* **2003**, *300*, 112. (c) Wu, Y.; Xiang, J.; Yang, C.; Lu, W.; Lieber, C. M. *Nature* **2004**, *430*, 61.
- (7) (a) *Chem. Mater.* **2004**, *16*, 4381–4846 (special issue on organic electronics). (b) Malliaras, G.; Friend, R. H. *Phys. Today* **2005**, May, 53.
- (8) (a) Sirringhaus, H.; Kawase, T.; Friend, R. H.; Shimoda, T.; Inbasekaran, M.; Wu, W.; Woo, E. P. *Science* **2000**, *290*, 2123. (b) Rogers, J. A.; et al. *Proc. Natl. Acad. Sci. U.S.A.* **2001**, *98*, 4835.
- (9) (a) Laquindanum, J. G.; Katz, H. E.; Lovinger, A. J.; Dodabalapur, A. *Chem. Mater.* **1996**, *8*, 2542. (b) Dimitrakopoulos, C. D.; Brown, A. R.; Pomp, A. J. *Appl. Phys.* **1996**, *80*, 2501. (c) Gundlach, D. J.; Lin, Y. Y.; Jackson, T. N.; Nelson, S. F.; Schlom, D. G. *IEEE Electron Dev. Lett.* **1997**, *18*, 87. (d) Klauk, H.; Schmid, G.; Radlik, W.; Weber, W.; Zhou, L. S.; Sheraw, C. D.; Nichols, J. A.; Jackson, T. N. *Solid-State Electron.* **2003**, *47*, 297.

- (10) (a) Steinhart, M.; Wendorff, J. H.; Greiner, A.; Wehrspohn, R. B.; Nielsch, K.; Schilling, J.; Choi, J.; Gosele, U. *Science* **2002**, *296*, 1997. (b) Steinhart, M.; Wehrspohn, R. B.; Gosele, U.; Wendorff, J. H. *Angew. Chem., Int. Ed.* **2004**, *43*, 1334. (c) Ginzburg-Margau, M.; Fournier-Bidoz, S.; Coombs, N.; Ozin, G. A.; Manners, I. *Chem. Commun.* **2002**, 3022. (d) O'Brien, G. A.; Quinn, A. J.; Iacopino, D.; Pauget, N.; Redmond, G. J. *Mater. Chem.* **2006**, *16*, 3237. (e) O'Brien, G. A.; Quinn, A. J.; Tanner, D. A.; Redmond, G. *Adv. Mater.* **2006**, *18*, 2379.
- (11) (a) Zhao, L.; Yang, W.; Ma, Y.; Yao, J.; Li, Y.; Liu, H. *Chem. Commun.* **2003**, 2442. (b) Gan, H.; Liu, H.; Li, Y.; Liu, Y.; Lu, F.; Jiu, T.; Zhu, D. *Chem. Phys. Lett.* **2004**, *399*, 130. (c) Qu, L.; Shi, G. *Chem. Commun.* **2004**, 2800. (d) Al-Kaysi, R. O.; Bardeen, C. J. *Chem. Commun.* **2006**, 1224.
- (12) Steinhart, M.; Zimmermann, S.; Goring, P.; Schaper, A. K.; Gosele, U.; Weder, C.; Wendorff, J. H. *Nano Lett.* **2005**, *5*, 429.
- (13) (a) Steinhart, M.; Jia, Z. H.; Schaper, A. K.; Wehrspohn, R. B.; Gosele, U.; Wendorff, J. H. *Adv. Mater.* **2003**, *15*, 706. (b) Luo, Y.; Lee, S. K.; Hofmeister, H.; Steinhart, M.; Gosele, U. *Nano Lett.* **2004**, *4*, 143.
- (14) Luo, Y.; Szafraniak, I.; Zakharov, N. D.; Nagarajan, V.; Steinhart, M.; Wehrspohn, R. B.; Wendorff, J. H.; Ramesh, R.; Alexe, M. *Appl. Phys. Lett.* **2003**, *83*, 440.

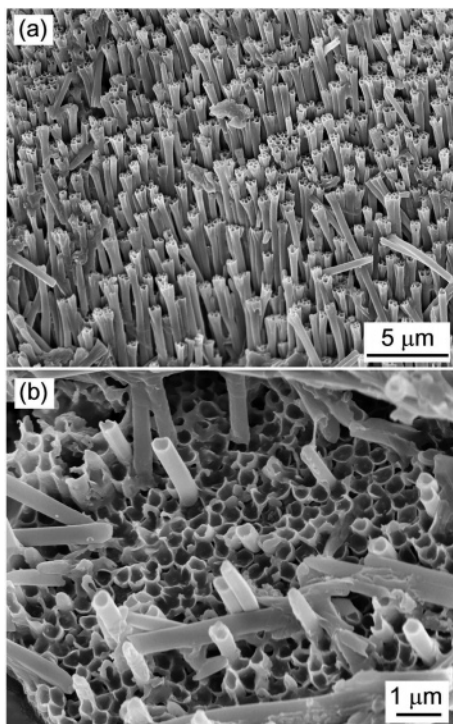


Figure 1. (a) SEM image of a pentacene nanotube array following template removal. (b) Higher magnification image of part of the back side of the membrane used in part (a) following partial template removal.

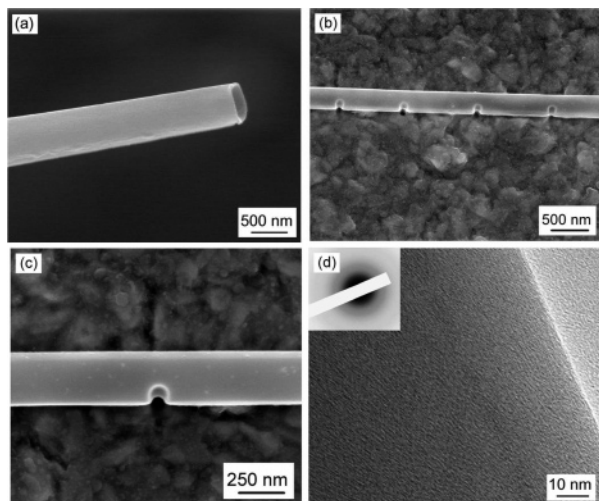


Figure 2. (a) High-resolution tilted SEM image of the end of a single pentacene nanotube. (b) Tilted SEM image of a pentacene “nanoflute” formed by local FIB milling. (c) Magnified image of a single hole from the nanoflute shown in part b. (d) TEM image of a pentacene nanotube showing texturing. Inset: Selected area electron diffraction data. The disk-like regions suggest a lack of long-range order within the tubes.

substrate and sputter coated with an ultrathin gold layer (~ 5 nm) to facilitate high-resolution imaging. In order to investigate whether the hollow structure was maintained along the length of the nanotubes, local structure editing using focused ion beam (FIB) milling was employed on single pentacene nanotubes dispersed onto gold substrates. Figure 2b shows a SEM image of the central section of a pentacene nanotube following spatially resolved FIB milling of a series of pits in order to open a series of holes along the tube. This “nanoflute” demonstrates that the tubular characteristics persist along the length of these 1-D nanostructures. Figure 2c shows a magnified image of a milled

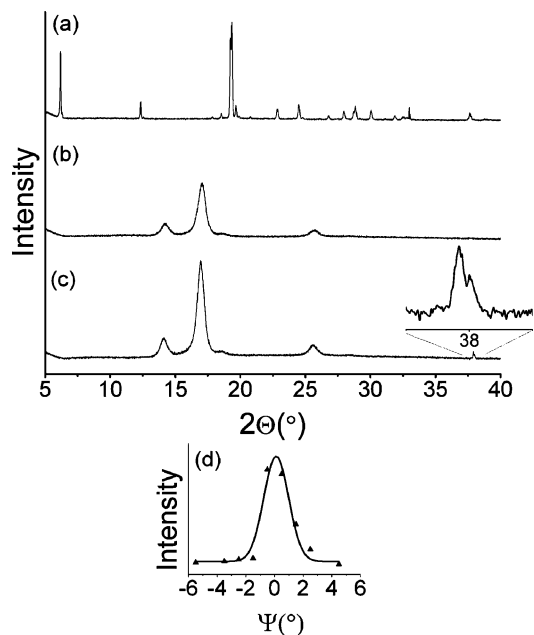


Figure 3. Θ - 2Θ XRD data acquired for (a) a thick film of pentacene prepared by melting pentacene powder, (b) a blank alumina template, and (c) an array of pentacene nanotubes embedded in an alumina template. Inset: magnified view of the nanotube peak observed at $2\Theta = 37.9^\circ$. (d) Rocking-angle (Ψ) data (triangles) acquired for this peak. The curve shows a Gaussian fit to the data, with full width at half-maximum $w_{\text{fwhm}} \approx 1.7^\circ$.

hole. Figure 2d shows a high-resolution TEM image of a single nanotube. The surface appears textured, suggesting a certain degree of molecular organization. In the selected area electron diffraction image shown in the inset neither diffraction spots nor rings are evident, indicating that the pentacene molecules within the tube do not adopt any appreciable long-range order. The disk-like features in the diffraction pattern suggest a liquid-like structure, where only short-range molecular correlations are present.¹⁵

In order to further characterize the structural properties of the synthesized nanotubes, X-ray diffraction (XRD) measurements were carried out on pentacene nanotube arrays embedded in porous alumina membranes; see Supporting Information. To investigate the thermal stability of pentacene during melt wetting, XRD data were first acquired for a thick film of pentacene, prepared under similar conditions to the melt-wetted nanotubes; see Figure 3a. The strong peak observed in the Θ - 2Θ scan at $2\Theta = 6.17^\circ$ corresponds to a $d(001)$ value of 14.4 \AA , characteristic of the pentacene bulk phase.¹⁶ A weaker peak centered at $2\Theta = 6.3^\circ$ indicates the presence of a second pentacene polymorph, with a corresponding $d(001)$ value of 14.1 \AA .¹⁶ Peaks observed at larger 2Θ values correspond to $d(00l)$ peaks ($l = 2-6$), together with a strong peak at $2\Theta = 19.3^\circ$, which corresponds to the $d(110)$ reflection.^{16a} All of these peaks show splitting (see Supporting Information, Figure S2) indicating the presence of two pentacene polymorphs in the thick film.¹⁶ Figure 3b shows a Θ - 2Θ X-ray diffractogram of an empty alumina

(15) (a) Eiermann, R.; Parkinson, G. M.; Bassler, H.; Thomas, J. M. *J. Phys. Chem.* **1983**, *87*, 544. (b) Siwick, B. J.; Dwyer, J. R.; Jordan, R. E.; Miller, R. J. D. *Science* **2003**, *302*, 1382.

(16) (a) Mattheus, C. C. Ph.D. Dissertation, University of Groningen, Groningen, The Netherlands, 2002. (b) Mattheus, C. C.; Bros, A. B.; Baas, J.; Oostergetel, G. T.; Meetsma, A.; de Boer, J. L.; Palstra, T. M. *Synth. Met.* **2003**, *138*, 475.

membrane. Three broad peaks are evident, centered at $2\Theta = 14.3^\circ$, 17.1° , and 25.9° , respectively, in agreement with literature reports.¹⁷

Figure 3c shows a diffractogram acquired for an array of pentacene nanotubes embedded in an alumina membrane. In addition to the three peaks observed for the blank membrane in Figure 3b, a weaker peak with maximum intensity at $2\Theta = 37.9^\circ$ was also observed; see Figure 3c (inset). This peak corresponds to the $d(006)$ peak for the thick film data shown in Figure 3a with a d spacing of $d \approx 2.37 \text{ \AA}$. The absence of the lower angle $d(00l)$ reflections, together with this small d spacing, suggests short-range herringbone-like packing with the long axes of pentacene molecules lying parallel to the pore long axis.^{16a} Rocking-angle (Ψ) scans were then performed in order to investigate the degree of molecular alignment within the nanotubes. Ψ is defined as the angle between the scattering vector and the sample surface normal; see Supporting Information, Figure S1. Figure 3d shows rocking-angle data acquired as a function of Ψ for successive scans of the $2\Theta = 37.9^\circ$ peak shown in the inset to Figure 3c. For each scan, the maximum peak intensity was plotted against Ψ . Fitting the acquired data to a Gaussian line shape yielded a full width at half-maximum value, $w_{\text{fwhm}} \approx 1.7^\circ$. The correlation length (L_{corr}) associated with this reflection can be calculated from w_{fwhm} by means of the Debye–Scherrer method, yielding $L_{\text{corr}} \approx 5 \text{ nm}$; see Supporting Information. The appearance of the $2\Theta = 37.9^\circ$ reflection for the pentacene nanotubes and the angular dependence of its intensity suggests short-range alignment of the pentacene molecules. Thus, both the electron diffraction and the XRD data indicate a lack of long-range order within the nanotubes.

Single nanotubes were electrically contacted using two-terminal (source, drain) top-contact device configurations on a range of oxide substrates. Figure 4a,b show optical and tilted SEM images, respectively, of single nanotube devices fabricated by drop-deposition of well-dispersed nanotubes onto substrates, followed by thermal evaporation of arrays of square gold contact electrodes through a TEM grid shadow mask. Well-resolved electrode contacts to each nanotube are clearly visible. Single nanotube devices were fabricated on oxidized silicon substrates for electrical characterization under ambient conditions. Figure 4c shows measured current–voltage (I – V) characteristics for two typical devices (1 and 2). For both devices, the data are linear and quasi-symmetric for low bias voltages ($-2.5 \text{ V} < V < 2.5 \text{ V}$). In this regime, the extracted device resistances (R_i , $i = 1, 2$) are $R_1 = 10 \pm 1 \text{ T}\Omega$ and $R_2 = 22 \pm 2 \text{ T}\Omega$. For these devices, the measured wire lengths (L_i) were $L_1 = 3.3 \mu\text{m}$ and $L_2 = 4.2 \mu\text{m}$. Taking the mean measured values for the nanotube

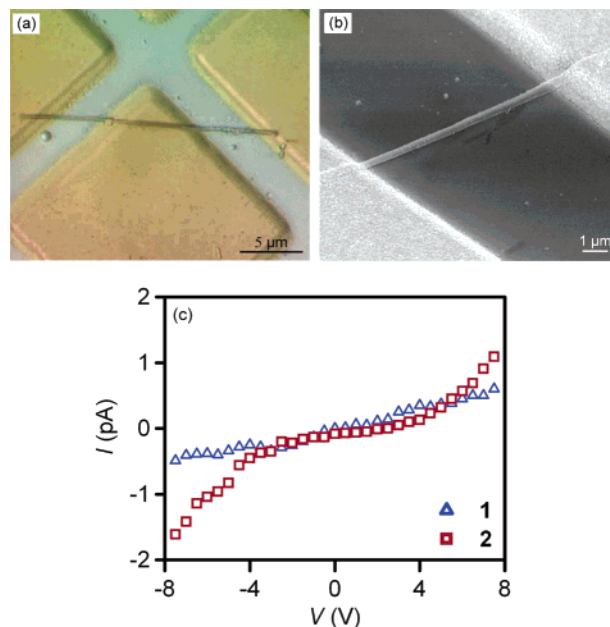


Figure 4. (a) Optical and (b) tilted SEM images of top-contacted single pentacene nanotube devices fabricated on oxidized aluminum substrates. (c) I – V data for two single nanotube devices fabricated on oxidized silicon substrates.

outer diameter ($D \approx 350 \text{ nm}$) and mean wall thickness ($W \approx 40 \text{ nm}$), the nanotube resistivity can be calculated, $\rho_i = \pi R_i [D^2 - (D - W)^2] / 4L_i$. This yields resistivity values $\rho_1 \approx 3 \times 10^5 \Omega \cdot \text{m}$ and $\rho_2 \approx 5 \times 10^5 \Omega \cdot \text{m}$. The measured I – V data for the single pentacene nanotubes shown in Figure 4c display nonlinear behavior at higher bias (particularly for device 2), suggesting an injection barrier at the gold–pentacene interface, in agreement with photoemission spectroscopy data obtained for interfaces between pentacene and gold.¹⁸

In summary, we have presented a convenient synthesis of pentacene nanotubes with good uniformity for key parameters such as tube length, outer diameter, and wall thickness. While initial structural data indicate an absence of long-range order within the tubes, preliminary two-terminal electrical characterization of single nanotube devices yielded resistivities $\sim 5 \times 10^5 \Omega \cdot \text{m}$. Ongoing work is directed toward optimizing synthesis and processing methods for demonstration of a single nanotube transistor.

Acknowledgment. This work was supported by the EU under the “Nano3D” project (STRP-014006) and by the Irish HEA PRTL Nanoscience Initiative.

Supporting Information Available: Experimental methods for nanotube synthesis and purification and also structural and electrical characterization. Expanded XRD data (PDF). This material is available free of charge via the Internet at <http://pubs.acs.org>.

CM0622654

(17) Guo, Y.-G.; Li, C.-J.; Wan, L.-J.; Chen, D.-M.; Wang, C.-R.; Bai, C.-L.; Wang, Y.-G. *Adv. Funct. Mater.* **2003**, *13*, 626.

(18) Watkins, N. J.; Yan, L.; Gao, Y. *Appl. Phys. Lett.* **2002**, *80*, 4384.